Journal of Molecular Catalysis A: Chemical 411 (2016) 337–343

Contents lists available at ScienceDirect

Journal of Molecular Catalysis A: Chemical

journal homepage: www.elsevier.com/locate/molcata

Effect of positive-charges in diphosphino-imidazolium salts on the structures of Ir-complexes and catalysis for hydroformylation

Heng Zhang, Yong-Qi Li, Peng Wang, Yong Lu, Xiao-Li Zhao, Ye Liu *

Shanghai Key Laboratory of Green Chemistry and Chemical Processes, School of Chemistry and Molecular Engineering, East China Normal University, Shanghai 200062, PR China

ARTICLE INFO

Article history:
Received 21 September 2015
Received in revised form 9 November 2015
Accepted 9 November 2015
Available online 15 November 2015

Keywords:
Ionic phosphines
Diphosphines
Ionic iridium complexes
Hydroformylation
Homogeneous catalysis

ABSTRACT

The effect of positive charges in the diphosphino-imidazolium salts of **L2** was investigated in terms of coordinating character, structures of corresponding Ir-complexes and catalysis for hydroformylation. It was found that the involved positive charges exhibited strong electron-withdrawing effect on the neighbored phosphine fragment, rendering **L2** more π-acceptor ability than the corresponding neutral counterpart of **L1**. Consequently, the changed coordinating ability of **L1** and **L2** led to the variety in the structures and components for the Ir-complexes (**Ir-L1a**, **Ir-L1b**, **Ir-L2a**, and **Ir-L2b**). The complexation of **L2** with Ir(acac)$(CO)_2$ led to a novel five-coordinate Ir(II)-complex of **Ir-L2a** chelated by a PCC (phosphine–carboanion–carbene) pincer in tripodal mode, whereas the complexation of **L1** with Ir(acac)$(CO)_2$ led to a four-coordinate square-planar Ir(I)-complex of **Ir-L1a** chelated by a PCP (phosphine–carboanion–phosphine) pincer. In addition, the different catalytic performances of these Ir-complexes ligated by **L1** and **L2** for hydroformylation of olefins were investigated.

1. Introduction

In transition metal catalyzed homogeneous catalysis, ligands as well as transition metals play significantly important roles in promoting the efficiency of the organic transformations [1]. Hydroformylation of olefins is one of the most important industrial processes relying on homogeneous catalysis with 100% atom economy [1,2]. The catalytic activity of the unmodified transition metals for hydroformylation is generally in the ranking of Rh » Co > Ir, Ru > Os > Pt > Pd » Fe > Ni, in which rhodium is the most efficient catalysts for this reaction [3]. Comparatively, despite of the economic advantages over rhodium, iridium-catalysts remain relatively less developed due to their much lower catalytic activity towards hydoformylation of olefins, as well as the competing hydrogenation of olefins to unwanted alkanes [4–10]. More recently, Beller and cowokers had reported a promising result for hydroformylation of a variety of olefins over a PPh_3-modified Ir-catalyst which was no more than 8 times slower than its Rh-counterpart [4]. Besides of the applied transition metals, the selection of ligands such as trivalent phosphines is another dominant method for improvement of reaction rates and selectivity. Hence, a great deal of work has been devoted to the ligand design [11,12].

In contrast to the electron-rich phosphine ligands as strong σ-donors [13,14], the electron-deficient ligands as π-acceptors also attracted much attention due to the involved π-backdonation from transition metals which corresponds to the unique performance for homogenous catalysis. For example, the uses of Rh-complexes with the π-acceptor ligands have been reported to be more active and more selective catalysts for hydroformylation [15–18]. The typical examples of electron-deficient ligands are phosphites and fluoroarylphosphines. However, P—O bonds of phosphites are instable and sensitive to hydrolysis [18] and the structural diversity for fluoroarylphosphines with stable P-C linkages is limited [19–21]. Recently, the phosphine salts in which the positive charges are vicinal to the P(III)-atoms of the phosphine fragments become attractive candidates for mimicking the π-acceptor ligands due to their advantages of the robustness and facile preparation. The phosphino-imidazolium salts have been firstly developed by Canac and Chauvin for the synthesis of the ionic transition metal complexes [22–29] and then applied to homogeneous catalysis by us [30–34].

In this paper, the diphosphine of **L1** and its ionic counterpart of **L2** derived from quaternization of **L1** by MeOTf were firstly prepared according to the reported methods [24,30]. Then they were used to develop the novel Ir-complexes (**Ir-L1a**, **Ir-L1b**, **Ir-L2a** and

* Corresponding author. Fax: +86 21 62233424.
E-mail address: yliu@chem.ecnu.edu.cn (Y. Liu).

http://dx.doi.org/10.1016/j.molcata.2015.11.005
1381-1169/

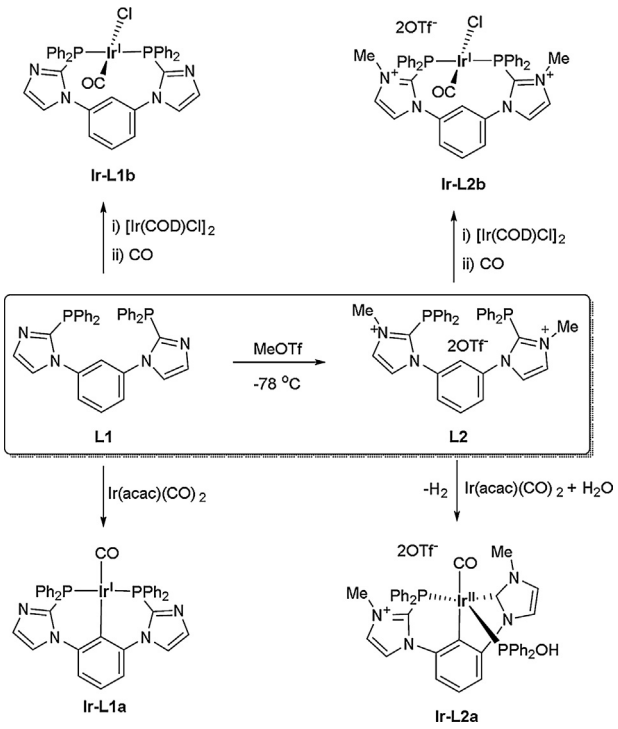

Scheme 1. Synthesis of the Ir-complexes (**Ir-L1a**, **Ir-L1b**, **Ir-L2a** and **Ir-L2b**) ligated by the neutral diphosphine of **L1** and the diphosphino-imidazolium salts of **L2** respectively.

Ir-L2b) as well as applied to catalyze hydroformylation of olefins. The effect of positive charge on the coordinating ability of **L2** and the catalysis for hydroformylation were investigated for the first time in comparison to those over **L1** with typical σ-donor ability (Scheme 1).

2. Experimental

2.1. Reagents and analysis

THF were dried and distilled over sodium/benzophenone, while dichloromethane were dried over CaH_2 and DMSO were dried over anhydrous sodium sulphate. All other reagents were purchased from Shanghai Aladdin Chemical Reagent Co. Ltd., and Alfa Aesar China, and used as received. All reactions were carried out under nitrogen atmosphere, using Schlenk and vacuum line techniques. The following analytical instruments were used. FT-IR spectra were recorded on a Nicolet NEXUS 670 spectrometer. The ^{1}H, ^{13}C NMR and ^{31}P NMR spectra for the analyses of the common compounds were recorded on a Bruker Avance 400 spectrometer. The ^{31}P NMR spectra for the analyses of the phosphine-selenides were recorded on a Bruker Avance 500 spectrometer at ambient temperature. The ^{31}P NMR spectra were referenced to 85% H_3PO_4 sealed in a capillary tube as an internal standard. Elemental analyses (CHN) were obtained by using an Elementar Vario EL III instrument. Gas chromatography (GC) was performed on a SHIMADZU-2014 equipped with a DM-1 capillary column (30 m × 0.25 mm × 0.25 μm). GC-mass spectrometry (GC–MS) was recorded on an Agilent 6890 instrument equipped with an Agilent 5973 mass selective detector.

2.2. Synthesis

*2-(Diphenylphosphanyl)-1-{3-[2-(diphenylphosphanyl)-1H-imidazol-1-yl]phenyl}-1H-imidazole **(L1)***

L1 was prepared according to the procedures reported by Chauvin [24] and us [30] with some modifications.

A solution of 1, 3-dibromobenzene (4.718 g, 20 mmol), imidazole (2.996 g, 44 mmol), K_2CO_3 (8.293 g, 60 mmol) and CuI (0.762 g, 4 mmol) in DMSO (50 mL) was stirred vigorously at 120 °C for 48 h. The reaction mixture after cooling to room temperature was filtered to give a clear solution which was treated with CH_2Cl_2 (300 mL) and deionized water (300 mL) to give an organic-aqueous biphasic solution. The collected organic phase was stripped of the solvent under vacuum, and the obtained residue was purified by column chromatography on silica gel, using CH_2Cl_2/ethanol (30:1) as an eluent, to afford the product of 1,3-di-imidazolyl benzene as a white solid (3.0 g, yield of 71.3%).

Under nitrogen atmosphere, to the solution of 1,3-di-imidazolyl benzene (2.0126 g, 10 mmol) in dry THF (150 mL) cooled to −78 °C was added dropwise with N, N, N′, N′-tetramethylethylenediamine (TMEDA, 3.0 mL, 20 mmol) and n-BuLi (2.5 M in hexane, 8.8 mL, 22 mmol). The obtained mixture after stirring vigorously for 1 h, chlorodiphenylphosphine (PPh_2Cl, 4.953 g, 22 mmol) was added dropwise. The resultant mixture was stirred overnight with the reaction temperature increasing to ambient. After quenching excess *n*-BuLi with deionized water, the obtained oily mixture was removed of solvent in vacuo. The residue was purified by column chromatography on silica gel, using CH_2Cl_2/ethyl acetate (30:1) as an eluent, to yield **L1** as a white solid (2.53 g, 44%). ^{1}H NMR (400 MHz, δ, ppm, CD_3CN): δ = 7.47 (t, J = 8 Hz, 1H, H_{Ph}), 7.32–7.36 (m, 24H, H_{Ph+imi}), 7.26 (s, 2H, H_{imi}), 7.18 (s, 1H, H_{Ph}). ^{31}P NMR (162 MHz, δ, ppm, $CDCl_3$): δ = −28.2 (s, PPh_2). The ^{31}P NMR signal of **L1** (δ = −28.2 ppm) observed herein was consistent to the one reported by Chauvin [24] with two phosphine fragments located in *trans*-position but different to the one reported by us [30] with two phosphine fragments located in *cis*-position.

*2-(Diphenylphosphanyl)-1-{3-[2-(diphenylphosphanyl)-3-methyl-1H-imidazol-3-ium-1 yl]phenyl}-3-methyl-1H-imidazol-3-ium bistriflate (**L2**)*

L2 was prepared according to the reported procedures [24,30] with some modifications.

To a solution of **L1** (0.5793 g, 1 mmol) in CH_2Cl_2 (30 mL) cooled at −78 °C was added methyl-trifluoromethanesulfonate (0.3349 g, 2 mmol). The solution was stirred overnight with the reaction temperature increasing to ambient. After evaporation of the solvent under vacuum, the residue was recrystallized from CH_2Cl_2/Et_2O to yield **L2** as white solids (0.7 g, 77%). ^{1}H NMR (400 MHz, δ, ppm, CD_3CN): δ = 7.73 (s, 2H, H_{imi}), 7.64 (s, 2H, H_{imi}), 7.28–7.51 (m, 24H, H_{Ph}), 3.48 (s, 6H, NCH_3). ^{31}P NMR (162 MHz, δ, ppm, CD_3CN): δ = −21.10 (s, PPh_2).

*2-(Diphenylphosphino)-1-phenyl-1H-imidazole (**L3**)*

L3 was obtained with the yield of 73% according to the preparation procedures for **L1**. ^{1}H NMR (400 MHz, δ, ppm, CD_3COCD_3): δ = 7.46–7.49 (m, 8H, H_{Ph}), 7.33–7.34 (m, 8H, H_{Ph+imi}), 7.29 (s, 1H, H_{Ph}). ^{31}P NMR (162 MHz, δ, ppm, CD_3COCD_3): δ = −31.17 (s, PPh_2).

*2-(Diphenylphosphino)-3-methyl-1-phenyl-1H-imidazol-3-ium triflate (**L4**)*

L4 was obtained with the yield of 87% after the stoichiometric quaternization of **L3** by MeOTf according to the preparation procedures for **L2**. ^{1}H NMR (400 MHz, δ, ppm, CD_3COCD_3): δ = 8.11 (s, 1H, H_{imi}), 8.09 (s, 1H, H_{imi}), 7.44–7.57 (m, 15H, H_{Ph}), 3.69 (s, 3H, NCH_3). ^{31}P NMR (162 MHz, δ, ppm, CD_3COCD_3): δ = −20.7 (s, PPh_2).

*Ir-complex upon coordination of **L1** to Ir(acac)(CO)$_2$ **(Ir-L1a)***

Under nitrogen atmosphere, a solution of Ir(acac)(CO)$_2$ (38.2 mg, 0.11 mmol) in dry CH_2Cl_2 (3 mL) was added to a solution of **L1** (57.9 mg, 0.1 mmol) in dry CH_2Cl_2 (3 mL). The resultant mixture was stirred vigorously at room temperature for 5 min. Then *n*-hexane was added to precipitate the orange–yellow solids. The orange-yellow solids were collected after dryness under vacuum with the yield of 88% (70 mg). The sample suitable for

Table 1
Crystal data and structure refinement for **Ir-L1a**, **Ir-L1b, Ir-L2a** and **Ir-L2b.**

	Ir-L1a.CH_2Cl_2	**Ir-L1b**.H_2O	**Ir-L2a**	**Ir-L2b**
Empirical formula	$C_{37}H_{27}Ir_1N_4O_1P_2.CH_2Cl_2$	$C_{37}H_{28}Cl_1Ir_1N_4O_1P_2.H_2O_1$	$C_{39}H_{34}Ir_1N_4O_2P_2.2(CF_3SO_3)$	$C_{39}H_{34}Cl_1Ir_1N_4O_1P_2.2(CF_3SO_3)$
Formula weight	882.69	852.22	1142.98	1162.43
Crystal system	Monoclinic	Orthorhombic	Orthorhombic	Triclinic
Space group	$P2_1/c$	*Pbcn*	*Pbca*	*P*-1
a (Å)	13.0624(7)	26.2223(5)	16.1818(11)	12.8635(4)
b (Å)	17.2838(10)	18.4901(4)	20.7304(15)	13.8201(4)
c (Å)	16.2701(9)	28.9516(6)	26.5775(18)	13.9595(4)
α (^{0})	90	90	90	76.8250(10)
β (^{0})	108.816(2)	90	90	79.0570(10)
γ (^{0})	90	90	90	68.5560(10)
V (Å^3)	3477.0(3)	14037.3(5)	8915.6(11)	2233.47(11)
Z	4	16	8	2
d_{calc} (g cm^{-3})	1.686	1.609	1.703	1.728
μ (Mo-Kα) (mm^{-1})	4.123	4.010	3.241	3.293
T (K)	173(2)	296(2)	296(2)	296(2)
λ (A)	0.71073	0.71073	0.71073	0.71073
Total reflections	40121	159026	98932	26183
Unique reflections (R_{int})	6129 (0.0911)	12367 (0.0670)	7838 (0.0881)	7811 (0.0333)
R_1 [I > 2σ(I)]	0.0333	0.0354	0.0430	0.0306
wR_2 (all data)	0.0695	0.0835	0.1112	0.0896
F(000)	1736	6688	4520	1148
Goodness-of-fit on F^2	1.027	1.066	1.037	1.092

X-ray diffraction analysis was obtained by recrystallization from CH_2Cl_2/*n*-hexane. ^{1}H NMR (400 MHz, δ, ppm, CD_2Cl_2): δ = 7.56–7.61 (m, 8H, H_{Ph}), 7.34–7.43 (m, 14H, H_{Ph}), 7.27 (s, 2H, H_{imi}), 6.78 (t, *J* = 8 Hz, 1H, H_{Ph}), 6.70 (s, 1H, H_{imi}), 6.68 (s, 1H, H_{imi}). ^{31}P NMR (162 MHz, δ, ppm, CD_2Cl_2): δ = 11.69 (s, *P*Ph_2). ^{13}C NMR (125 MHz, δ, ppm, CD_2Cl_2): δ = 187.89 (t, *J* = 8.75 Hz, Ir-*C*O), 144.62 (t, *J* = 2.5 Hz, C_{Ar}), 142.18 (t, *J* = 13.75 Hz, C_{Ar}), 135.87 (t, *J* = 42.5 Hz, C_{Ar}), 134.45 (s, C_{Ar}), 132.07 (t, *J* = 5 Hz, C_{Ar}), 131.29 (s, C_{Ar}), 130.24 (t, *J* = 26.25 Hz, C_{Ar}), 128.53 (t, *J* = 6.25 Hz, C_{Ar}), 127.35 (s, C_{Ar}), 122.78 (s, C_{Ar}), 121.27 (s, C_{Ar}). CHN-elemental analysis (found): C 55.15, H 3.64, N 6.8 (calcd., C 55.70, H 3.41, N 7.02).

Ir-complex upon coordination of ***L1*** *to [Ir(cod)Cl]$_2$* ***(Ir-L1b)***

Ir-L1b. Under nitrogen atmosphere, a solution of $[Ir(cod)Cl]_2$ (33.6 mg, 0.05 mmol) in dry CH_2Cl_2 (2 mL) was stirred vigorously at room temperature for about 10 min. Then the atmospheric CO (in a balloon) was introduced into the reaction mixture for 20 min. Afterwards, the reaction mixture was treated with a solution of **L1** (57.9 mg, 0.1 mmol) in dry CH_2Cl_2 (3 mL). The resultant mixture was stirred for another 2.5 h and then *n*-hexane was added to precipitate the yellow solids. The yellow solids were collected after dryness under vacuum with the yield of 89% (74 mg). The sample suitable for X-ray diffraction analysis was obtained by slow volatilization from acetonitrile. ^{1}H NMR (400 MHz, δ, ppm, CD_3CN): δ = 8.49 (s, 1H, H_{Ph}), 8.28–8.33 (m, 4H, H_{Ph}), 7.68 (s, 2H, H_{Ph}), 7.44–7.54 (m, 11H, H_{Ph}), 7.37–7.38 (m, 6H, H_{Ph}), 7.14–7.15 (m, 4H, H_{imi}). ^{31}P NMR (162 MHz, δ, ppm, CD_3CN): δ = 5.19 (s, *P*Ph_2). ^{13}C NMR (125 MHz, δ, ppm, CD_2Cl_2): δ = 169.1 (s, Ir-*C*O), 141.32 (t, *J* = 42.5 Hz, C_{Ar}), 137.19 (s, C_{Ar}), 134.71 (t, *J* = 28.75 Hz, C_{Ar}), 132.47 (s, C_{Ar}), 131.53 (t, *J* = 6.25 Hz, C_{Ar}), 131.11 (d, *J* = 40 Hz, C_{Ar}), 128.95 (s, C_{Ar}), 128.66 (t, *J* = 6.25 Hz, C_{Ar}), 127.92 (t, *J* = 6.25 Hz, C_{Ar}), 127.55 (s, C_{Ar}), 126.24 (s, C_{Ar}). CHN-elemental analysis (found): C 53.35, H 3.52, N 6.26 (calcd., C 53.27, H 3.38, N 6.72).

Ir-complex upon coordination of ***L2*** *to Ir(acac)(CO)$_2$* ***(Ir-L2a)***

Under nitrogen atmosphere, a solution of **L2** (90.7 mg, 0.1 mmol) in dry CH_2Cl_2 (6 mL) was added to a solution of Ir(acac)$(CO)_2$ (41.7 mg, 0.12 mmol) in CH_2Cl_2 (4 mL) at 40 °C and the resultant mixture with presence of trace water was stirred vigorously for ca 2 h. Then diethyl ether was added to the reaction solution to precipitate the yellow solids, which were collected after dryness under vacuum with the yield of 65% (74 mg). The sample suitable for X-ray diffraction analysis was obtained by recrystallization from CH_2Cl_2/diethyl ether. Due to the paramagnetic nature for the Ir(II)-center complex-cation, the signals of ^{1}H NMR and ^{31}P NMR of **Ir-L2a** attributed to ligand **L2** were broadened to flatness. CHN-elemental analysis (found): C 42.67, H 3.24, N 4.62 (calcd., C 43.08, H 2.98, N 4.90).

Ir-complex upon coordination of ***L2*** *to* $[Ir(cod)Cl]_2$ *(**Ir-L2b**)*

Under nitrogen atmosphere, a solution of $[Ir(cod)Cl]_2$ (33.6 mg, 0.05 mmol) in dry CH_2Cl_2 (2 mL) was stirred vigorously at room temperature for about 10 min and then the atmospheric CO (in a balloon) was introduced into the reaction mixture for 20 min. The obtained mixture was then treated with a solution of **L2** (90.7 mg, 0.1 mmol) in acetonitrile (5 mL) and was stirred vigorously for about 4.5 h. Then diethyl ether was added to precipitate the yellow solids, which were collected after dryness under vacuum with the yield of 81% (94 mg). The sample suitable for X-ray diffraction analysis was obtained by recrystallization from acetonitrile/*n*-hexane. ^{1}H NMR (400 MHz, δ, ppm, CD_3CN): δ = 8.63 (t, *J* = 4 Hz, 1H, H_{Ph}), 8.05 (s, 2H, H_{imi}), 7.82–7.49 (m, 25H, H_{Ph+imi}), 3.27 (s, 6H, NCH_3). ^{31}P NMR (162 MHz, δ, ppm, CD_3CN): δ = 12.22 (s, PPh_2). ^{13}C NMR (125 MHz, δ, ppm, CD_3CN): δ = 167.49 (s, Ir-CO), 139.20 (t, *J* = 20 Hz, C_{Ar}), 136.27 (s, C_{Ar}), 135.39 (s, C_{Ar}), 134.06 (d, *J* = 26.25 Hz, C_{Ar}), 133.72 (t, *J* = 7.5 Hz), 130.66 (t, *J* = 6.25 Hz), 130.32 (quintet, *J* = 5 Hz, CF_3SO_3), 130.11 (s, C_{Ar}), 128.93 (s, C_{Ar}), 126.84 (t, *J* = 30 Hz, C_{Ar}), 126.37 (s, C_{Ar}), 123.31 (t, *J* = 27.5 Hz, C_{Ar}), 40.36 (s, NCH_3). CHN-elemental analysis (found): C 42.48, H 3.11, N 4.82 (calcd., C 42.36, H 2.93, N 4.82).

2.3. X-ray crystallography

Intensity data for **Ir-L1a**, **Ir-L1b**, **Ir-L2a** and **Ir-L2b** were collected on a Bruker SMARTAPEX II diffractometer using graphite monochromated Mo-Kα radiation (λ = 0.71073 Å). Data reduction included absorption corrections by the multi-scan method. The structures were solved by direct methods and refined by full matrix least-squares using SHELXS-97 (Sheldrick, 1990), with all non-hydrogen atoms refined anisotropically. Hydrogen atoms were added at their geometrically ideal positions and refined isotropically. The crystal data and refinement details are given in Table 1.

2.4. General procedures for hydroformylation of 1-octene

In a typical experiment, Ir-L1a (0.02 mmol, or the other Ir-complex), the ligand at the required amount, the solvent (2 mL)

were mixed with 1-octene (10 mmol) in a 50 mL sealed Teflon-lined stainless steel autoclave, which was pressured with syngas (CO/H_2 = 2:1, 4.0 MPa) and then stirred vigorously at 120 °C for 6 h. Upon completion, the autoclave was cooled down to room temperature, the pressure was carefully released. The solution was analyzed by GC to determine the conversions (*n*-dodecane as internal standard) and the selectivities (normalization method).

3. Results and discussion

3.1. Synthesis and characterization

It is believed that the magnitudes of $^1J_{Se-P}$ in the ^{77}Se isotopomer of the phosphine-selenides in ^{31}P NMR spectra can be used to measure the σ-donor ability of the corresponding phosphines [35–37]. An increase of $^1J_{Se-P}$ indicates an increase in the character of π-acceptor ability (i.e., less σ-donor ability) of a phosphine [36]. To estimate the σ-donor ability of **L1-L4**, their corresponding phosphine-selenides were prepared by reacting elemental selenium (with 7.63% ^{77}Se) with each phosphine in deuterated solvent under the appointed conditions (See condition described in Fig. 1), which were directly analyzed without isolation by a Bruker Avance 500 spectrometer at ambient temperature. It was indicated that the phosphine fragments in **L1-L4** and PPh_3 exhibited the π-acceptor ability in an order of **L2** ($^1J_{Se-P}$ = 782 Hz), **L4** (780 Hz) > **L1** ($^1J_{Se-P}$ = 751 Hz), **L3** ($^1J_{Se-P}$ = 753 Hz) > PPh_3 ($^1J_{Se-P}$ = 729 Hz). Evi-

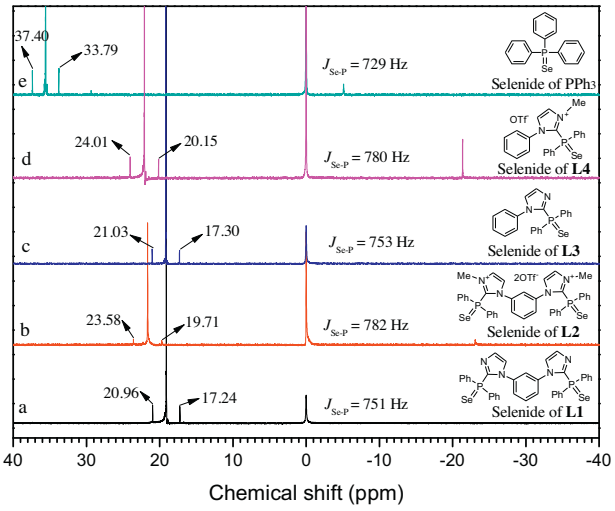

Fig. 1. ^{31}P NMR spectra of the selenides of **L1-L4** in comparison to that of PPh_3 (202 MHz): (a) reacting elemental selenium with **L1** in $CDCl_3$ at 70 °C for 10 h; (b) reacting elemental selenium with **L2** in DMSO-d_6 at 70 °C for 10 h; (c) reacting elemental selenium with **L3** in $CDCl_3$ at 70 °C for 10 h; (d) reacting elemental selenium with **L4** in $CDCl_3$ at 70 °C for 10 h; (e) reacting elemental selenium with PPh_3 in $CDCl_3$ at 70 °C for 10 h.

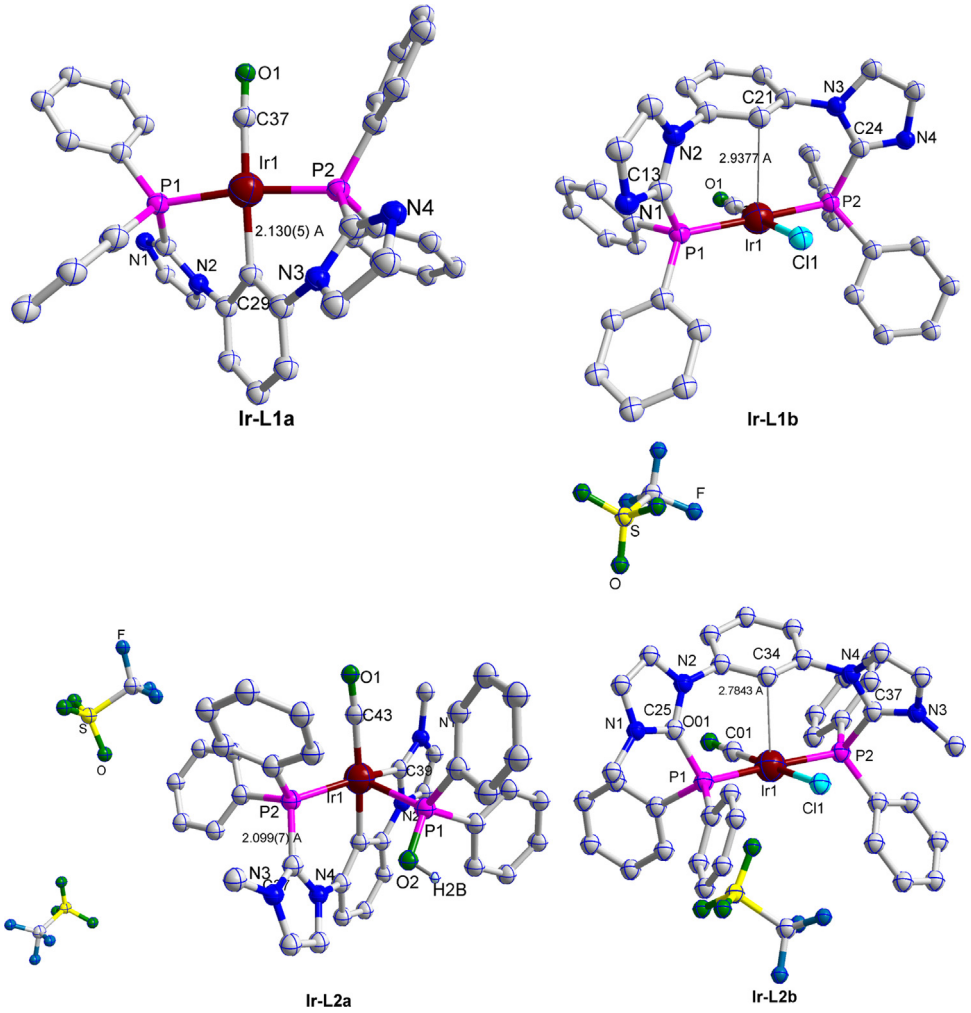

Fig. 2. The single crystal structures of the iridium complexes of **Ir-L1a**, **Ir-L1b**, **Ir-L2a** and **Ir-L2b** (The hydrogen atoms and solvent molecules are omitted for clarity).

Table 2
The selected bond distances, bond angles, vibrational frequency of CO (ν, cm^{-1}) in FT-IR spectra, and ^{31}P NMR signals for **Ir-L1a**, **Ir-L1b**, **Ir-L2a**, and **Ir-L2b.**

Ir-complex	Bond distance/Å				Bond angles/^{0}	ν (CO)/cm^{-1}	^{31}P NMR/ppm
	Ir-P	Ir -C_{CO}	Ir-C^-/carbene	Ir-Cl	P1-Ir-P2		
Ir-L1a	2.2770(14)2.2714(14)	1.849(6)	2.130(5)	–	170.94(5)	1978	11.69
Ir-L1b	2.3166(14)2.3104(15)	1.814(6)	–	2.3837(13)	176.35(5)	1981	5.19
Ir-L2a	2.2988(19)2.3870(18)	1.90(1)	2.099(7)2.058(7)	–	102.17(6)	2062	–
Ir-L2b	2.2913(11)2.3086(11)	1.825(5)	–	2.3739(12)	176.31(4)	1996	12.22

dently after the introduction of positive charge into **L1** or **L3** through selective quaternization at N-site of imidazolyl ring, the coordinating ability of the phosphine fragments in **L2** or **L4** changed dramatically, with indication of the dramatically increased magnitudes of $^1J_{Se\text{-}P}$ from 750 to 780 Hz.

Consequently, the resultant Ir-complexes ligated by **L1** and **L2** respectively are certainly different in structures and components. The molecular structures of the obtained Ir-complexes analyzed by the single crystal X-ray diffraction were depicted in Fig. 2. The complexation of Ir(acac)$(CO)_2$ with **L1** free of any additive led to the formation of **Ir-L1a** with the yield of 88% which possessed the typical square-planar geometry. The Ir(I) ($5d^8$) center, lying at the center of inversion, was coordinated by a PCP pincer in a square-planar chelating mode, as well as a CO ligand. The in situ generation of carboanion from meta-phenylene of **L1** with acetylacetonate ($acac^-$) in precursor of Ir(acac)$(CO)_2$ as a H^+-scavenger to afford a PCP pincer was the inherent driving force for the formation of **Ir-L1a** with the two fused six-member rings to Ir(I)-center, in which the shorter Ir-P bond distances [2.2770(14) and 2.2714(14) Å] was observed corresponding to the more consolidated Ir-P linkages and then the good thermodynamical stability. Interestingly, the complexation of Ir(acac)$(CO)_2$ with **L2** under the same conditions led to the formation of the ionic complex of **Ir-L2a** with the presence of trace water, which was composed of Ir(II)-complex cation and two OTf^- counteranions. In comparison to **Ir-L1a** as a four-coordinate complex, the complex cation of **Ir-L2a** was a five-coordinate one, in which the Ir(II) ($5d^7$) center, lying at the center of trigonal bipyramid, was coordinated by a PCC (phosphine-carboanion–carbene) pincer, and the other two ligands of CO and $(HO)PPh_2$. The chelation of the PCC-pincer to Ir-center in the mode of fused five-member and six-member rings was the thermodynamic driving force for the formation of **Ir-L2a**. Obviously, in ionic ligand **L2**, the deprotonation at 2C position of meta-phenylene to afford a carboanion and the heterolytic cleavage of one N_2C-P bond to give a transient *N*-heterocyclic carbene (NHC) along with the release of electrophilic P^+Ph_2 could result in a PCC pincer, which was the first example to trap the potential PCC tripodal pincer in a Ir(II)-complex along with the change of oxidation state of Ir-center from +1 to +2. In particular, the electron-withdrawing effect of the neighbored positive imidazoliums in **L2** not only makes the deprotonation at 2C position of meta-phenylene much easier to afford carboanion along with acetylacetonate as the H^+-scavenger, but also facilitate the generation of N-heterocyclic carbene (NHC) since the imidazolium-neighbored phosphine units can be regarded as the NHC-phosphenium adducts [24,25,29]. The concurrent released phosphenium of $^+PPh_2$ was hydrolysed to give $(HO)PPh_2$ as an accessible phosphinite ligand [29] to coordinate to Ir-center, and simultaneously the liberated H^+ from H_2O was reduced by Ir^+ ion to H_2 with the result of the formation of oxidative Ir^{2+} ion. Resultantly, in **Ir-L2a**, the complex cation counteracted by two OTf^- anions is in low-spin state with the paramagnetism due to the presence of one unpaired electron in Ir(II) ($5d^7$) center. Hence, the ^1H NMR and ^{31}P NMR signals attributed to **Ir-L2a** are broadened to flatness. In contrast to **Ir-L2a** complex, we had reported a Pd-complex in which the same PCC pincer induced from **L2** was trapped but without the concurrent coordination of $(HO)PPh_2$ to the metal center [33].

In contrast, the complexation of $[Ir(cod)Cl]_2$ dimer instead of Ir(acac)$(CO)_2$ with **L1** and **L2** respectively led to the formation of **Ir-L1b** (yields 89%) and **Ir-L2b** (yields 81%) which both possessed the typical square-planar geometry. The Ir(I) ($5d^8$) center, lying at the center of inversion, was coordinated by the diphosphine located in *trans*-positions, as well as a CO and a Cl^- ligands. However, without the presence of $acac^-$ as the suitable acid-scavenger, the generation of carboanion from meta-phenylene to afford a PCP pincer from **L1** (or **L2**) was unfavorable [28], and then the coordination of Cl^- to Ir-center became convenient to form **Ir-L1b** (or **Ir-L2b**), in which *cis*-positioned two $-PPh_2$ fragments projected inwards to be able to form a pocket around Ir-center, allowing **L1** (or **L2**) to develop P-Ir-P chelation in *trans*-position with bite angle of 176° due to the bulky bis(imidazolyl)-phenyl bridge in **L1** (or **L2**). However, the structural parameters in **Ir-L1b** and **Ir-L2b** were quite different (Table 2). As for **Ir-L2b**, the more consolidated interactions between Ir and P were observed [2.2913(11) and 2.3086(11) Å] due to the π-backdonation in Ir-P linkages derived from the intensive π-acceptor ability of **L2** ($^1J_{Se\text{-}P}$ = 782 Hz). This is consistent with the observed CO vibrational frequency of **Ir-L2b** (1996 cm^{-1}), which is

Table 3
Comparison of the catalytic performance of different iridium-complexes with or without the presence of auxiliary ligand for hydroformylation of 1-octene[a].

Entry	Complex	Ligand	P/Ir	Syngas (MPa)	Conv. (%)[b]	Sel. (%)[b]			L/B[c]	TON[d]
						Aldehydes	Hydrogenation products	Isomerization products		
1	**Ir-L1a**	–	2	4.0	42	68	31	1	3.3	143
2	**Ir-L1b**	–	2	4.0	89	62	26	11	3.3	276
3	**Ir-L2a**	–	2	4.0	35	45	35	20	2.7	80
4	**Ir-L2b**	–	2	4.0	91	30	50	20	2.6	140
5	**Ir-L1b**	**L3**	5	4.0	88	83	11	6	2.7	365
6	**Ir-L1b**	**L4**	5	4.0	85	70	19	11	3.3	299
7	**Ir-L2b**	**L3**	5	4.0	75	80	14	6	2.9	300
8	**Ir-L2b**	**L4**	5	4.0	21	51	44	5	3.1	54
9[e]	$Rh(CO)(PPh_3)_2Cl$	**L3**	5	4.0	84	72	5	23	1.5	1512

[a] Ir-concentration 0.2 mol% (Ir-complex 0.02 mmol), 1-octene 10.0 mmol, NMP (1-methyl-2-pyrrolidinone) 2 mL, syngas CO:H_2 = 2:1 (volume ratio), temp. 120 °C, time 6 h.
[b] Determined by GC.
[c] L/B, the ratio of linear nonanals to branched ones.
[d] TON, turnover number = mol of nonanals.(mol of Ir)-l.
[e] $Rh(CO)(PPh_3)_2Cl$ 0.04 mol%.

Table 4
Generality of Ir-L1b with the presence of L3 for hydroformylation of different olefins[a].

Entry	Substrate	Conv. (%)[b]	Sel. (%)[b]			L/B[c]	TON[d]
			Aldyhydes	Hydrogenation products	Isomerization products		
1	1-Hexene	87	95	3	2	2.3	423
2	Styrene	41	89	11	–	0.4	181
3	Cyclohexene	<5	–	–	–	–	–

[a] Ir-concentration 0.2 mol% (**Ir-L1b** 0.02 mmol), **L3** 0.06 mmol (P/Ir = 5 molar ratio), olefin 10.0 mmol, NMP 2 mL, syngas 4.0 MPa (CO:H_2 = 2:1, volume ratio), temp. 120 °C, time 6 h.
[b] Determined by GC.
[c] L/B, the ratio of linear aldehydes to branched ones.
[d] TON, turnover number = mol of aldehydes.(mol of Ir)-l.

bigger higher than **Ir-L1b** (1981 cm^{-1}). So the stability of the ionic complex of **Ir-L2b** was good enough to stand in open air for more than one month without decomposition.

3.2. Catalytic performance of Ir-complexes for hydroformylation of olefins

It is well known that the properties of a transition metal complex (in terms of the coordinating geometry, the valance state of metal center and the thermal stability) and the involved ligands with different electronic and steric effects dramatically influence the catalysis for organic transformations. In this part, the inherent catalytic performance of **Ir-L1(a, b)** and **Ir-L2(a, b)** and the effect of the auxiliary ligands (**L1-L4**) were investigated comparatively for hydroformylation of 1-octene. As summarized in Table 3 under the optimal conditions (120 °C, syngas 4.0 MPa, NMP as a solvent), **Ir-L1**(a, b) and **Ir-L2**(a, b) all showed moderate activities with TON in the ranking of **Ir-L1b** > **Ir-L2b**, **Ir-L1**a > **Ir-L2a** (Entries 1–4). Obviously, the ones with square-planar geometry (**Ir-L1b** and **Ir-L2**b) exhibited higher activities than the chelated **Ir-L1a** and **Ir-2a**. The latters ligated by the PCP- and PCC-pincer respectively would be unfavorable to the dissociation of the involved ligands to form the active Ir-species and then impede the accommodation of the substrates (CO and 1-octene), leading to the poorer transformation of 1-octene to nonanals.

In addition, compared to **Ir-L1b**, **Ir-L2b** exhibited a worse chemoselectivity in terms of nearly the same conversion of 1-octene with much lower aldehyde formation (Entry 2 vs 4). Interestingly, the involvement of **L3** was found to be able to both improve the chemoselectivity to nonanols with TON increased from 276 up to 365 over **Ir-L1b** and 140 to 300 over **Ir-L2b**, indicating the role of **L3** to suppress isomerization and hydrogenation (Entry 2 vs 5; Entry 4 vs 7). In comparison, TON of 365 over **Ir-L1**b/**L3** system was just ca. 5 times lower than the corresponding $Rh(CO)(PPh_3)_2Cl$/**L3** one (TON = 1512) on the benchmark of the same yield of nonanals (Entry 5 vs 9).

The reaction data over **Ir-L1b** and **Ir-L2b** indicated that even with the similar structure and the same Ir^+ center, the changed coordinating ability for **L2** because of the introduction of the positive charges could definitely result in the different catalytic performance for hydroformylation. The relatively stronger σ-donor of **L1** ($^1J_{Se\text{-}P}$ = 751 Hz) exhibited better catalytic performance in comparison to **L2** with less σ-donor ability ($^1J_{Se\text{-}P}$ = 782 Hz) (Entry 2 vs 4). And the involvement of **L3** with relatively strong σ-donor ability ($^1J_{Se\text{-}P}$ = 753 Hz) further improved the catalytic performance of **Ir-L1b** with the highest TON of 365 (Entry 5), and **Ir-L2b** with the TON of 300 (Entry 7). Comparatively, the weak σ-donor ability of **L4** corresponded to the decreased efficiency for hydroformylation (Entries 6 and 8). Especial in Entry 8, the combination of **L2** and **L4** both with the weak σ-donor ability (**L2**, $^1J_{Se\text{-}P}$ = 782 Hz; **L4**, $^1J_{Se\text{-}P}$ = 780 Hz) led to the poor transformation in terms of 1-octene conversions and aldehyde selectivities (TON = 54).

It was found that **Ir-L1**b/**L3** also exhibited well activity towards the hydroformylation of 1-hexene and styrene, but inert to cyclohexene (Table 4).

4. Conclusions

The introduction of positive charge(s) into a phosphine was indeed a feasible methodology to develop the robust π-acceptor ligands. The intensive electron-withdrawing effect of the positive-charges rendered the neighboured phosphine fragments more π-acceptor ability such as in **L2** and **L4**. The phosphine fragments in **L1-L4** and PPh_3 exhibited π-acceptor ability in an order of **L2** ($^1J_{Se\text{-}P}$ = 782 Hz), **L4** ($^1J_{Se\text{-}P}$ = 780 Hz) > **L1** ($^1J_{Se\text{-}P}$ = 751 Hz), **L3** ($^1J_{Se\text{-}P}$ = 753 Hz) > PPh_3 ($^1J_{Se\text{-}P}$ = 729 Hz). The different coordinating ability of **L1** and **L2** consequently led to the variety in the structures and components for the Ir-complexes (**Ir-L1a**, **Ir-L1b**, **Ir-L2a** and **Ir-L2b**). The complexation of **L2** with $Ir(acac)(CO)_2$ afforded a novel five-coordinate Ir(II)-complex of **Ir-L2a** chelated by a PCC (phosphine–carboanion–carbene) pincer in tripodal mode, whereas the complexation of **L1** with $Ir(acac)(CO)_2$ led to a four-coordinate square-planar Ir(I)-complex of **Ir-L1a** chelated by a PCP (phosphine–carboanion–phosphine) pincer. The different Ir-complexes in terms of structures and components consequently corresponded to the different catalytic performance for hydroformylation of olefins. It was found that the PCP-chelated **Ir-L1a** and PCC-chelated **Ir-2a** exhibited the worse activities towards hydroformylation than **Ir-L1b** and **Ir-L2b** with square-planar geometry. Even for **Ir-L1b** and **Ir-L2b** with the same structures and Ir^+-center, and the similar components, their catalytic performance varied greatly because of the changed coordinating ability of **L1** and **L2**. The relatively stronger σ-donor of **L1** ($^1J_{Se\text{-}P}$ = 751 Hz) exhibited better catalytic performance than **L2** with less σ-donor ability.

Acknowledgments

This work was financially supported by the National Natural Science Foundation of China (Nos.21473058, 21273077, and 21076083), and 973 Program from Ministry of Science and Technology of China, (2011CB201403).

References

[1] R. Franke, D. Selent, A. Börner, Chem. Rev. 112 (2012) 5675–5732.
[2] P.W.N.M. Van Leeuwen, C. Claver, Rhodium-Catalyzed Hydroformylation, Kluwer, Dordrecht, 2000.
[3] F.P. Pruchnik, Organometallic Chemistry of Transition Elements, Plenum Press, New York, 1990.
[4] I. Piras, R. Jennerjahn, R. Jachstell, A. Spannedberg, R. Franke, M. Beller, Angew. Chem. Int. Ed. 50 (2011) 280–284.
[5] C.M. Crudden, H. Alper, J. Org. Chem. 59 (1994) 3091–3097.
[6] E. Mieczyńska, A.M. Trzeciak, J.J. Ziółkowski, I. Kownacki, B. Marciniec, J. Mol. Catal. A: Chem. 237 (2005) 246–253.
[7] M.A. Moreno, M. Haukka, T.A. Pakkanen, J. Catal. 215 (2003) 326–331.
[8] A.B. Permin, R. Eisenberg, J. Am. Chem. Soc. 124 (2002) 12406–12407.
[9] D.J. Fox, S.B. Duckett, C. Flaschenriem, W.W. Brennessel, J. Schneider, A. Gunay, R. Eisenberg, Inorg. Chem. 45 (2006) 7197–7209.

[10] M. Rosales, J.A. Durán, A. González, I. Pacheco, R.A. Sánchez-Delgado, J. Mol. Catal. A: Chem. 270 (2007) 250–256.
[11] V.V. Grushin, Chem. Rev. 104 (2004) 1629–1662.
[12] S.H. Chikkali, J.I. Van der Vlugt, J.N.H. Reek, Chem. Rev. 262 (2014) 1–15.
[13] S. Wurtz, F. Glorius, Acc. Chem. Res. 41 (2008) 1523–1533.
[14] S. Díez-González, S.P. Nolan, Angew. Chem. Int. Ed. 46 (2007) 2988–3000.
[15] X.F. Wu, X.J. Fang, L.P. Wu, R. Jackstell, H. Neumann, M. Beller, Acc. Chem. Res. 47 (2014) 1041–1053.
[16] O. Diebolt, H. Tricas, Z. Freixa, P.W.N.M. van Leeuwen, ACS Catal. 3 (2013) 128–137.
[17] S. Aguado-Ullate, J.A. Baker, V. González-González, C. Müller, J.D. Hirst, J.J. Carbó, Catal. Sci. Technol. 4 (2014) 979–987.
[18] H. Tricas, O. Diebolt, P.W.N.M. van Leeuwen, J. Catal. 298 (2013) 198–205.
[19] C.L. Pollock, G.C. Saunders, E.C.M.S. Smyth, V.I.J. Sorokin, Fluor. Chem. 129 (2008) 142–166.
[20] M.L. Clarke, D. Ellis, K.L. Mason, A.G. Orpen, P.G. Pringle, R.L. Wingad, D.A. Zaher, R.T. Baker, Dalton Trans. 7 (2005) 1294–1300.
[21] S. Jeulin, S. Duprat de Paule, V. Ratovelomanana-Vidal, J.P. Genêt, N. Champion, P. Dellis, Angew. Chem. Int. Ed. 43 (2004) 320–325.
[22] R. Chauvin, Eur. J. Inorg. Chem. 4 (2000) 577–591.
[23] N. Debono, Y. Canac, C. Duhayon, R. Chauvin, Eur. J. Inorg. Chem. 19 (2008) 2991–2999.
[24] Y. Cnanc, N. Debono, L. Vendier, R. Chauvin, Inorg. Chem. 48 (2009) 5562–5568.
[25] M. Azouri, J. Andrieu, M. Picquet, H. Cattey, Inorg. Chem. 48 (2009) 1236–1242.
[26] Y. Canac, N. Debono, C. Lepetit, C. Duhayon, R. Chauvin, Inorg. Chem. 50 (2011) 10810–10819.
[27] Y. Canac, C. Maaliki, I. Abdellah, R. Chauvin, N. J. Chem. 36 (2012) 17–27.
[28] C. Barthes, C. Lepetit, Y. Canac, C. Duhayon, D. Zargarian, R. Chauvin, Inorg. Chem. 52 (2013) 48–58.
[29] I. Abdellah, C. Lepetit, Y. Canac, C. Duhayon, R. Chauvin, Chem. Eur. J. 16 (2010) 13095–13108.
[30] Y.Q. Li, P. Wang, H. Zhang, X.L. Zhao, Y. Lu, Z. Popović, Y. Liu, J. Mol. Catal. A: Chem. 402 (2015) 37–45.
[31] H.X. You, Y.Y. Wang, X.L. Zhao, S.J. Chen, Y. Liu, Organometallics 32 (2013) 2698–2704.
[32] S.J. Chen, Y.Y. Wang, W.H. Yao, X.L. Zhao, G. VO-Thanh, Y. Liu, J. Mol. Catal. A: Chem. 378 (2013) 293–298.
[33] J. Zhang, Y.Y. Wang, X.L. Zhao, Y. Liu, Eur. J. Inorg. Chem (2014) 975–985.
[34] C.L. Zhou, J. Zhang, M. Đaković, Z. Popović, X.L. Zhao, Y. Liu, Eur. J. Inorg. Chem. 21 (2012) 3435–3440.
[35] D.W. Allen, B.F. Taylor, Dalton Trans. 1 (1982) 51–54.
[36] A. Suárez, M.A. Méndez-Rojas, A. Pizzano, Organometallics 21 (2002) 4611–4621.
[37] B. Milde, D. Schaarschmidt, T. Rüffer, H. Lang, Dalton Trans. 41 (2012) 5377–5390.